

LA-UR- 04-0624

Approved for public release;
distribution is unlimited.

Title: STACKING FAULT AND TWINNING IN
NANOCRYSTALLINE METALS

Author(s): Xiaozhou Liao
Yonghao Zhao
Srinivasan Srivilliputhur
Fei Zhou
Enrique J Lavernia
Michael I Baskes
Huifang Xu, Yuntian Zhu

Submitted to: 2004 TMS Annual Meeting



Los Alamos

NATIONAL LABORATORY

Los Alamos National Laboratory, an affirmative action/equal opportunity employer, is operated by the University of California for the U.S. Department of Energy under contract W-7405-ENG-36. By acceptance of this article, the publisher represents and warrants that the U.S. Government retains a nonexclusive, royalty-free license to publish or reproduce the published form of this contribution, or to allow others to do so, for U.S. Government purposes. Los Alamos National Laboratory requests that the publisher identify this article as work performed under the auspices of the U.S. Department of Energy. Los Alamos National Laboratory strongly supports academic freedom and a researcher's right to publish; as an institution, however, the Laboratory does not endorse the viewpoint of a publication or guarantee its technical correctness.

STACKING FAULT AND TWINNING IN NANOCRYSTALLINE METALS

X.Z. Liao,¹ Y.H. Zhao,¹ S.G. Srinivasan,¹ F. Zhou,² E.J. Lavernia,² M.I. Baskes,¹ H.F. Xu,³
and Y.T. Zhu¹

¹Materials Science and Technology Division, Los Alamos National Laboratory
Los Alamos, NM 87545

²Department of Chemical Engineering & Materials Science, University of California
Davis, CA 95616

³Department of Earth & Planetary Sciences, University of New Mexico
Albuquerque, NM 87131

Abstract

Nanocrystalline Al processed by cryogenic ball-milling and nanocrystalline Cu processed by high-pressure torsion at a very low strain rate and at room temperature were investigated using high-resolution transmission electron microscopy. For nanocrystalline Al, we observed partial dislocation emission from grain boundaries, which consequently resulted in deformation stacking faults and twinning. We also observed deformation twins formed via two other mechanisms recently predicted by molecular dynamic simulations. These results are surprising because (1) partial dislocation emission from grain boundaries has not been experimentally observed although it has been predicted by simulations and (2) deformation stacking faults and twinning have not been reported in Al due to its high stacking fault energy. For nanocrystalline Cu, we found that twinning becomes a major deformation mechanism, which contrasts with the literature reports that deformation twinning in coarse-grained Cu occurs only under high strain rate and/or low temperature conditions and that reducing grain sizes suppresses deformation twinning. The investigation of the twinning morphology suggests that twins and stacking faults in nanocrystalline Cu were formed through partial dislocation emissions from grain boundaries. This mechanism differs from the pole mechanism operating in coarse-grained Cu.

Keywords: nanocrystalline, Aluminum, copper, deformation mechanisms, twinning, stacking faults.

Introduction

Nanocrystalline materials have been reported to have superior mechanical properties such as high strength, which can coexist with very good ductility [1-3]. These superior mechanical properties are attributed to their unique deformation mechanisms, which are fundamentally different from those in their coarse-grained (CG) counterparts [4-8]. Some deformation mechanisms, e.g., partial dislocation emission from grain boundaries (GBs) or free surfaces, heterogeneous twinning nucleated from GBs, and twin lamellae formed via the dissociation and migration of GBs, have been predicted to operate in nanocrystalline (nc) face-centered-cubic (fcc) metals by molecular-dynamics simulations. Our recent experimental results [9-12] have confirmed many deformation mechanisms predicted by molecular dynamic simulations for nc fcc metals. In this paper, we review the results on our recent high-resolution transmission electron microscopy (HREM) investigation of the deformation mechanisms in nanocrystalline Al and Cu.

Experimental Procedures

Al sample: Al powder with a purity of ~ 99.9 wt% (Valimet) was ball milled in liquid nitrogen. The starting powder consists of equiaxed particles with diameters of 0.5 to 1 μm . The ball-milling was performed in a modified Union Process 1-S attritor (Szegvari) with a stainless steel vial and stainless steel balls (6.4mm in diameter) as milling media. Detailed description on the ball-milling process can be found in ref. 9. The iron content did not show measurable increase after the ball milling, indicating little contamination from the milling media. However, there could be contamination from C, N, H and O.

Cu sample: A 99.99 wt.% pure CG Cu disk with a thickness of 0.5 mm and a diameter of 10 mm was processed into nc Cu via high-pressure torsion (HPT) [13] for 5 revolutions under 7 GPa at room temperature and a very low strain rate of about 10^{-2} s^{-1} . HPT produces 100% dense nc materials without introducing any impurity into deformed samples.

The ball-milled Al powder was pressed to form a small pellet and then mechanically ground and ion-milled. The Cu disk was first cut into a size smaller than 3 mm in diameter and then mechanically ground to a thickness of about 10 μm followed by subsequent ion-milling. HREM investigation was carried out using a JEOL 3000F microscope operated at 300 kV.

Results and Discussion

(1) Ball-milled Al powder

The as-milled Al powder contains both elongated and equiaxed grains. The diameters of most equiaxed grains and the widths of most elongated grains are smaller than 100 nm. Figure 1 shows HREM images of (a) stacking faults (SFs) (marked by arrows), (b) the atomic level image of a typical SF, and (c) a deformation twin in nc Al. On (111) slip planes that have a path length for dislocation motion of ~50 nm SFs are observed (Fig. 1a). The SF density is $6 \times 10^{14} \text{ m}^{-2}$. In contrast, on $(11\bar{1})$ planes with a path length of ~150 nm, only full dislocations at a high-density of $3 \times 10^{16} \text{ m}^{-2}$ are observed. The SFs are formed by the grain boundary emission of leading and trailing Shockley partials, which is consistent with the molecular dynamics simulation [14]. In addition, the partial dislocation emission depends on the dislocation path length on the slip planes on which they glide. This result suggests a transition from full dislocation slip to partial dislocation slip with decreasing grain size. The SF width (Fig. 1b) was likely affected by both resolved nucleation stress [15] and the diffusion of impurities to the SF after ball-milling. Figure 1c shows a deformation twin with a thickness of two atomic planes. Such twins are formed by the dynamic overlapping of two extended partial dislocations with SFs on adjacent slip planes [14]. As shown, the two SFs are only partially overlapped. This twinning mechanism is different from the well-known pole mechanism.

Figure 2 shows (a) a TEM image of a twin at the right corner of a grain with the twin boundary marked by two white arrows, and (b) a HREM image of the twin. The twin was likely formed by the heterogeneous mechanism proposed by Yamakov et al [14]. Specifically, the twin was likely nucleated at the right corner of the grain and grew larger via the emission of Shockley partial dislocations from the GB. As shown, the whole right corner on the right of the twin boundary has been transformed into a twin. It is not clear if the first partial dislocation was emitted at the very bottom of the corner, but further growth of the twin shown in Fig. 2 can only

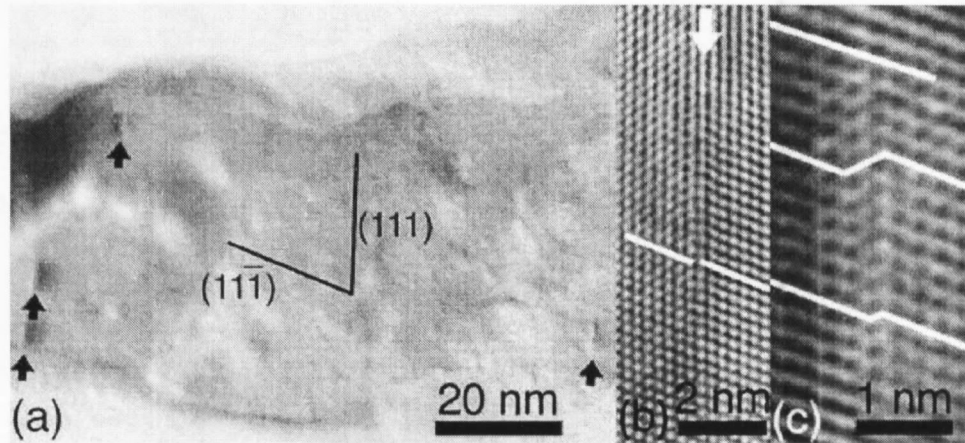


Figure 1. (a) SFs on (111) planes, which are marked by black arrows. Only full dislocations were observed on $(11\bar{1})$ planes, which have a much longer path length than the (111) planes; (b) atomic level image of a typical SF; and (c) a deformation twin formed by the overlapping of two extended dislocations on adjacent slip planes.

occur by partial dislocation emission at a plane above and adjacent to the twin boundary, which moves the twin boundary upward. MD simulations indicate that at very fine grain sizes (e.g. <8 nm), GB sliding and GB diffusion are the primary deformation mechanisms [4,16,17]. At larger grain sizes (e.g. 8-45 nm), partial dislocations emitted from GBs contribute significantly to the deformation [6-7, 14-15]. The MD simulations usually predict very high critical shear stresses of a few GPa for partial dislocations to emit from GBs, because of very high strain rates used in MD simulations. However, a recent analytical model [18] predicted much lower critical shear stresses of a few hundred MPa at lower strain rates that are closer to the experimental conditions of ball milling. Below 15 nm the model [18] indicates that partial dislocations are emitted at a stress lower than the stress needed for emitting full dislocations. Therefore, partial dislocation emission from GBs is a viable deformation mechanism under the ball-milling conditions in this study.

Note that the twin in Fig. 2 is located at a small corner of a much larger grain of several tens nanometers. According to the MD simulations [4,14,17], it would be very difficult for this grain to slide against another grain because of its large size, and partial dislocation emission from GBs is a major deformation mechanism. On the other hand, the twin boundary has a length of 14 nm, which is also the length of the slip plane. The slip plane length determines whether a partial or full dislocation is emitted from the GB. As the lengths of all slip planes below the twin boundary in Fig. 2b are shorter than 14 nm, the partial dislocation emission from GBs was the primary deformation mode. Therefore, it is logical to conclude that the twin in Fig. 2 was formed by the successive emission of partial Shockley dislocations from GBs on adjacent slip planes.

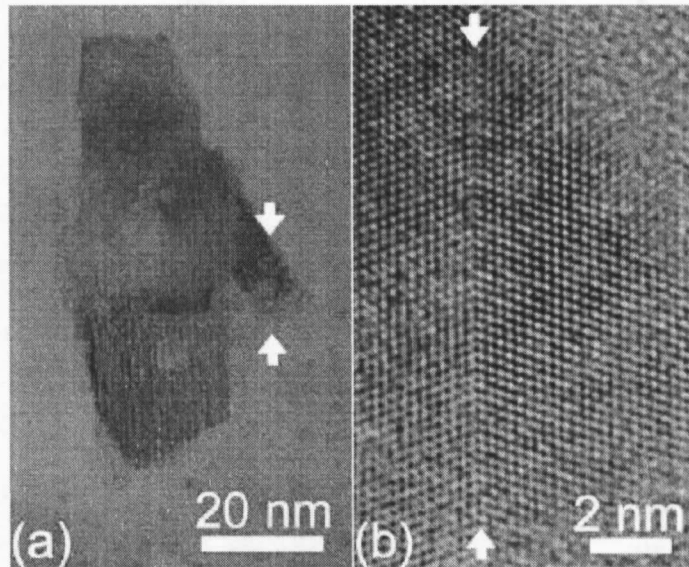


Figure 2. (a) A deformation twin at the right corner of a large grain with the twin boundaries marked by two white arrows, and (b) a HREM image of the twin.

Figure 3a shows another type of twin. The insert in Fig. 3a shows the Fourier transformation of a region that encompasses areas A and B. It demonstrates that the two areas form a crystallographic twinning relationship with $(1\bar{1}1)$ as the twinning plane. However, the boundary between area A and area B is wavy instead of the usual straight twinning plane characteristic of conventional twins. In fact, sharp, straight boundaries are the features that are often used to identify twins in a low magnification TEM micrograph or optical photograph. Figure 3b is an atomic scale image of the twinning boundary enlarged from the white frame in Fig. 3a. It indicates that areas A and B indeed form a twin relationship. Some segments of the boundary are straight, coherent $(1\bar{1}1)$ twin boundaries as indicated by white arrows. These segments, which are connected by non-crystallographic segments, form a zigzag boundary between the two twinning areas. Examination of the local twinning morphology in Fig. 3b reveals that the twin strikingly resembles a type of twin observed in the MD simulation [14]. This type of twins is formed by an entirely different mechanism, which involves the splitting and subsequent migration of a GB segment, leaving behind two coherent twin boundaries. This mechanism was first proposed by Ashby and Harper [19] in 1967 and was subsequently discussed by Gleiter [20]. It appears that the twin shown in Fig. 3 was formed by this mechanism. More specifically, a GB segment was dissociated into a twin boundary and a new GB [14]. A twin lamella was formed via the migration of the new GB. The boundaries of twin lamellae formed at different time frames joined together to form the zigzag boundary between areas A and B. The non-crystallographic segments observed here were actually the new GBs in this mechanism. Readers are referred to the work by Yamakov et al [14] for more detailed description on the twinning mechanism.

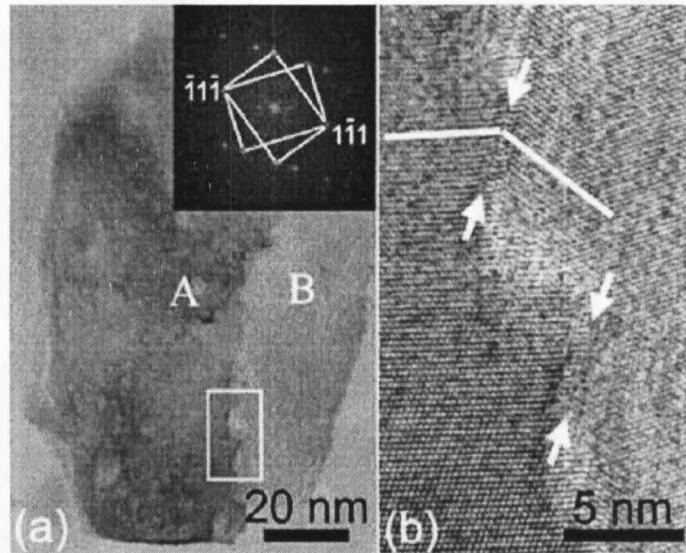


Figure 3. (a) Areas A and B form a twinning relationship with a wavy boundary between them. The insert shows Fourier transformation of a region that encompasses areas A and B, which indicates a $(1\bar{1}1)$ twinning plane; b) HRTEM image of a twin boundary segment from the white frame in (a). It consists of short, straight, coherent $(1\bar{1}1)$ twinning planes (marked by arrows) connected by incoherent, non-crystallographic segments.

Deformation twinning and stacking faults have never been reported in CG Al due to the very high stacking fault energy of Al. Therefore, the above observations are surprising and they demonstrate that when the size scale is reduced down to the nano range, nature will facilitate deformation via mechanisms that are not accessible at conventional length scale.

(2) HPT Cu disk

Investigation in the HPT Cu sample suggests that the deformation of the Cu disk is not uniform with the disk center being least deformed and the disk edge having the finest grain sizes. In some place of the Cu disk, part of a sub-micron-sized grain has been transformed into nc grains while the other part remains a large grain. A typical example is shown in a $\langle 110 \rangle$ HREM image in Fig. 4a. It is interesting to note that, while there is no twin in the part that remains a large grain (see the right part in Fig. 4a), microtwins and stacking faults are seen everywhere in the nanocrystalline area in Fig. 4a. To see the microtwin HREM image more clearly, an area indicated by a black rectangle in Fig. 4a is enlarged and shown in Fig. 4b. It is seen that the whole area is in an exact $\langle 110 \rangle$ zone-axis although the area has been divided into a few nanocrystalline grains. Grain boundaries in Fig. 4b are highlighted using black stars. The $\{111\}$ planes that form the twin relationship in the middle nanocrystalline grain are indicated using black lines. The twin widths and mirror plane positions between the middle and the upper grains are different while there is no twin in the lower grain in Fig. 4b, implying the twins were formed after the formation of those nanocrystalline grains, which is consistent with the fact that no twin is seen in large grains in the sample.

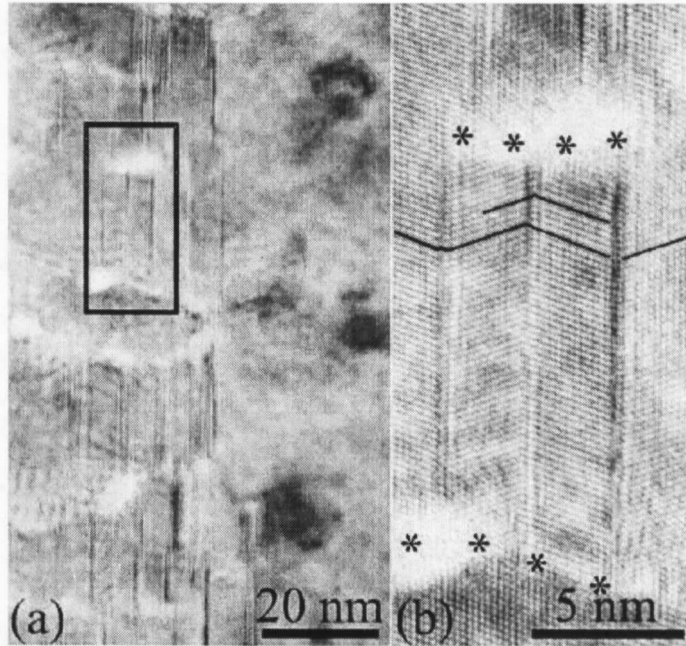


Figure 4. (a) A $\langle 110 \rangle$ HREM image of a grain in which the left part of the grain has been transferred into elongated nanocrystalline grains while the right part still remains a sub-micron-sized grain; (b) a magnified image of the part indicated by a black-rectangle in (a).

The experimental observation of the deformation twinning in nc Cu contradicts the literature reports: (1) it has been suggested that both the critical slip stress and twinning stress follow the Hall-Petch relationship, with the Hall-Petch slope for twinning (k_T) significantly larger than that for slip (k_S) for many CG metals and alloys [21]. For Cu the k_T is about $0.7 \text{ MN/m}^{3/2}$ while k_S is about $0.35 \text{ MN/m}^{3/2}$ [22]. Consequently, dislocation slip rather than deformation twinning is expected to become the preferred deformation mode when the grain is smaller than a certain size. Indeed, Meyers et al. [23] reported that shock compression at 35 GPa produced abundant deformation twins in Cu samples with grain sizes of 117 and 315 μm but virtually no twinning in a Cu sample with a grain size of 9 μm ; and (2) CG Cu does not deform by twinning [24,25] except at very high strain rate [26,27] and/or low temperature [28].

The contradiction between our experimental observation and the literature reports may imply that the twinning mechanism in nc Cu is different from that in CG Cu. Indeed, we found the twinning in nc Cu occurs through partial dislocation emission from GBs. Figure 5a shows a typical twinning morphology in an elongated grain observed from $[011]$. Most of the twin planes are $(11\bar{1})$ (indicated by white arrows) and one twin plane is $(\bar{1}\bar{1}1)$ (indicated by a black arrow). High density of micro-twins and stacking faults are seen in areas marked A, B, and C, respectively. The area B, where the narrowest $(11\bar{1})$ planes are less than 10 nm in width, is magnified in Fig. 5b. There is only one twin boundary at the right part of Fig. 5b that divides twin domains I and II. However, there are high densities of micro-twins and stacking faults, which can also be regarded as micro-twins with the thickness of only one atomic layer, at the left part of II. These micro-twins and stacking faults do not pass across the whole grain but stop in the grain interior with Shockley partial dislocations located at the front boundaries of the micro-twins and stacking faults. It is obvious that these twins were heterogeneously nucleated

at a grain boundary and grew into the grain interior via partial dislocation emissions from the GB.

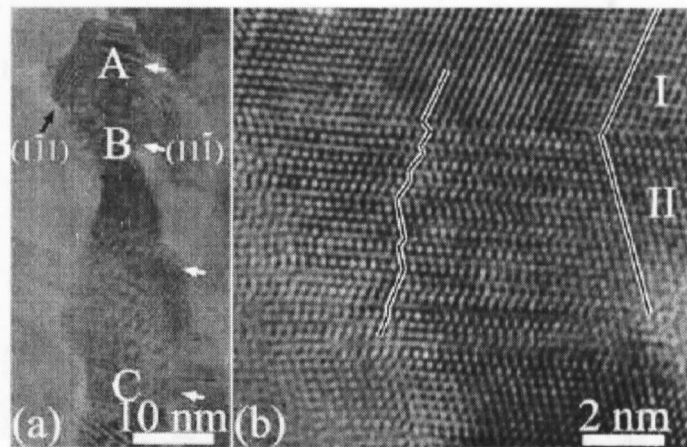


Figure 5. (a) A typical [011] HRTEM image of an elongated crystallite with width varying from smaller than 10 nm to about 20 nm. Twins are seen in this crystallite with most of the twin planes being $(11\bar{1})$ (indicated by white arrows) and one being $(\bar{1}\bar{1}1)$ (indicated by a black arrow). Micro-twins and stacking faults are seen in areas marked A, B, and C, respectively; (b) an enlarged image of area B in (a). The right part of the image shows only two twin domains: I and II, while the left part of II have a lot of micro-twins and stacking faults with one end of the micro-twins/stacking faults stops within the crystallite.

The above experimental observations demonstrate that Cu can deform by twinning at a very low strain rate and room temperature if its grain size is in the nanometer range. The grain size effect on deformation twinning in CG Cu, i.e. smaller grains are less likely to twin, does not apply to nc Cu. Our results suggest that the deformation twinning in nc Cu is due to the grain size effect, i.e. caused by the unique deformation mechanism in nc Cu. In CG Cu, deformation twinning is generally believed to occur via the pole mechanism and requires higher resolved shear stresses that can only be reached under high strain rate and/or low temperature conditions. In contrast, in nc Cu deformation twins form via partial dislocation emission from grain boundaries instead of the pole mechanism. Therefore, the Hall-Petch relationship for twinning does not apply to the nc Cu. More specifically, in nc Cu the conventional dislocation source (e.g. the Frank-Reed source) in the grain interior may no longer operate and even no longer exist. As a consequence, dislocations need to be emitted from the grain boundaries. Smaller grains make it easier to emit partial dislocations than to emit perfect dislocations from grain boundaries [6]. This makes partial dislocation emission from grain boundaries a major deformation mechanism when the grain size is below a certain critical value, and explains the pervasive deformation twins observed in this study.

Conclusion

Nanocrystalline Al and Cu have been found to deform via mechanisms that are not accessible at conventional length scale. In particular, twinning via partial dislocation emissions from GBs becomes a major deformation mechanism in nc Al and Cu. The unique deformation

mechanisms in nc metals will definitely affect the mechanical behavior of the nc metals.

Acknowledgements

This work was supported by the US DOC IPP Program Office and the Office of Naval Research (Grants Nos. N00014-02-1-1053 and N00014-03-1-0149).

References

1. R.Z. Valiev, I.V. Alexandrov, Y.T. Zhu, and T.C. Lowe, *J. Mater. Res.* 17 (2002), 5-8.
2. X. Zhang, H. Wang, R.O. Scattergood, J. Narayan, C.C. Koch, A.V. Sergueeva, and A.K. Mukherjee, *Appl. Phys. Letts.* 81 (2002), 823-825.
3. D. Jia, Y.M. Wang, K.T. Ramesh, E. Ma, Y.T. Zhu, and R.Z. Valiev, *Appl. Phys. Letts.* 79 (2001), 611-613.
4. J. Schiøtz, F. D. DiTolla, K. W. Jacobsen, *Nature* 391 (1998), 561-563.
5. K.S. Kumar, S. Suresh, M.F. Chisholm, J.A. Horton, and P. Wang, *Acta Mater.* 51 (2003), 387-405.
6. H. Van Swygenhoven, *Science* 296 (2002), 66-67.
7. V. Yamakov, D. Wolf, S.R. Phillpot, A.K. Mukherjee, and H. Gleiter, *Nature Materials* 1 (2002), 45-48.
8. M.W. Chen, E. Ma, K.J. Hemker, H.W. Sheng, Y.M. Wang, X.M. Cheng, *Science* 300 (2003), 1275-1277.
9. X.Z. Liao, F. Zhou, E.J. Lavernia, S.G. Srinivasan, M.I. Baskes, D.W. He and Y.T. Zhu, *Appl. Phys. Lett.* 83 (2003), 632-634.
10. X.Z. Liao, F. Zhou, E.J. Lavernia, D.W. He, and Y.T. Zhu, *Appl. Phys. Lett.* 83 (2003), 5062-5064.
11. X.Z. Liao, J.Y. Huang, Y.T. Zhu, F. Zhou, and E.J. Lavernia *Phil. Mag.* 83 (2003), 3065-3075.
12. X.Z. Liao, Y.H. Zhao, S.G. Srinivasan, Y.T. Zhu, R.Z. Valiev and D.V. Gunderov, *Appl. Phys. Lett.*, in press.
13. R.Z. Valiev, R.K. Islamgaliev, I.V. Alexandrov, *Prog. Mater. Sci.* 45 (2000), 103-189.
14. V. Yamakov, D. Wolf, M. Salazar, S.R. Phillpot, and H. Gleiter, *Acta Mater.* 50 (2002), 5005-5020.
15. V. Yamakov, D. Wolf, S.R. Phillpot, and H. Gleiter, *Acta Mater.* 49 (2002), 2713-2722.
16. M. Murayama, J.M. Howe, H. Hidaka, and S. Takaki, *Science* 295 (2002), 2433-2435.
17. H. Van Swygenhoven, M. Spaczer, A. Caro, and D. Farkas, *Phys. Rev. B* 60 (1999) 22-25.
18. R.J. Asaro, P. Krysl, and B. Kad, *Philos. Mag. Lett.* (in press).
19. M.F. Ashby, E. Harper, *Harvard Rept. Sept.* (Harvard University Press, Cambridge, MA, 1967)
20. M.A. Meyers, O. Vöhringer, and V.A. Lubarda, *Acta Mater.* 49 (2001), 4025-4039.
21. H. Gleiter, *Progress in Materials Science*, edited by J.W. Christian, P. Haasen, and T.B. Massalski (Pergamon, Oxford, 1981), Clalmers-Anniversary Volume, p. 17.
22. O. Vöhringer, *Z. Metallk.* 67 (1976), 518-524.
23. M.A. Meyers, U.R. Andrade, and A.H. Chokshi, *Metall. Mater. Trans.* 26A (1995), 2881-2893.
24. C.D. Liu, M.N. Bassim, and D.X. You, *Acta Metall. Mater.* 42 (1994), 3695-3704.
25. N. Hansen and B. Ralph, *Acta Metall.* 30 (1982), 411-417.
26. O. Johari and G. Thomas, *Acta Metall.* 2 (1964), 1153.
27. C.S. Smith, *Trans. Met. Soc. AIME.* 212 (1958), 574-589.
28. T.H. Blewitt, R. Coltman, and J.K. Redman, *J. Appl. Phys.* 28 (1957), 651-660.